A dicarbazole–triazine hybrid bipolar host material for highly efficient green phosphorescent OLEDs

ARTICLE *in* JOURNAL OF MATERIALS CHEMISTRY · FEBRUARY 2012

Impact Factor: 7.44 · DOI: 10.1039/C2JM14686J

11 AUTHORS, INCLUDING:

Chih-Hao Chang
Yuan Ze University
69 PUBLICATIONS **1,784** CITATIONS
SEE PROFILE

Ken-Tsung Wong
National Taiwan University
261 PUBLICATIONS **8,093** CITATIONS
SEE PROFILE

Raymond C. Kwong
Universal Display Corporation
57 PUBLICATIONS **4,471** CITATIONS
SEE PROFILE

Chihaya Adachi
Kyushu University
364 PUBLICATIONS **15,536** CITATIONS
SEE PROFILE

Journal of Materials Chemistry

Cite this: J. Mater. Chem., 2012, 22, 3832

www.rsc.org/materials

PAPER

A dicarbazole–triazine hybrid bipolar host material for highly efficient green phosphorescent OLEDs

Chih-Hao Chang,*[a] Ming-Cheng Kuo,[b] Wei-Chieh Lin,[a] Yu-Ting Chen,[a] Ken-Tsung Wong,*[b] Shu-Hua Chou,[b] Ejabul Mondal,[b] Raymond C. Kwong,[c] Sean Xia,[c] Tetsuya Nakagawa[d] and Chihaya Adachi[d]

Received 21st September 2011, Accepted 13th December 2011
DOI: 10.1039/c2jm14686j

A novel bipolar host material 9-(4,6-diphenyl-1,3,5-triazin-2-yl)-9′-phenyl-3,3′-bicarbazole (**CzT**) comprising a dicarbazole donor linking to an electron deficient 1,3,5-triazine acceptor was synthesized and characterized. The molecular design of **CzT** allows the spatial separation of HOMO and LUMO on the donor and acceptor moieties, respectively, giving sufficient triplet energy (2.67 eV) together with promising physical properties and morphological stability ($T_g = 134$ °C). This tailor-made material was used as a host for an efficient yellowish-green iridium complex, bis(*o*-tolylpyrimidinato-*N*,$C^{2\prime}$)Ir(III) acetylacetonate [$(TPm)_2$Ir(acac)]; the as-fabricated phosphorescent OLEDs (PHOLEDs) demonstrated high performance, with maximum efficiencies of 20.0% (75.7 cd A^{-1} and 71.3 lm W^{-1}) and 20.1% (76.3 cd A^{-1} and 72.7 lm W^{-1}) achieved in trilayer and bilayer device architectures, respectively. The efficiency of the trilayer device can sustain ~20% over a wide brightness range from 10^2 to 10^3 cd m^{-2} due to the more effective confinement of emissive excitons within the emitting layer.

Introduction

Phosphorescent OLEDs (PHOLEDs) have become the subject of intensive investigation in recent years because of their tremendous potential in both display and lighting applications.[1,2] Electro-phosphorescence can efficiently make full use of both the singlet and triplet excited states, rendering the internal quantum efficiency the ideal level of 100%.[3–5] Apparently, the use of the host–guest strategy with triplet emitters (guest) dispersed homogeneously within a suitable organic matrix (host) gives PHOLEDs the unity internal quantum efficiency due to the suppression of triplet–triplet annihilation, which is detrimental to the efficiency of triplet emitters. After years of research efforts, both the efficiencies and lifetimes of PHOLEDs have improved significantly. Particularly, the red emission of the commercially available active matrix OLED display is now dominated by phosphorescence. It is reasonable to envision the green phosphors will also take over from the green fluorescent emitters in the near future. As such, there exists intense demand for the development of new green host materials. In general, charge transport and charge balance are the two crucial factors for high-efficiency OLEDs.[6,7] One promising strategy for carrier balance is to incorporate an electron-donating moiety (donor, D) and an electron-withdrawing moiety (acceptor, A) into a single bipolar host material.[8] However, the molecular design strategy employed to incorporate the individual characteristics of D and A components while simultaneously retaining a reasonably large triplet energy to prevent the reverse energy transfer effect[9–11] is crucial. Some recent examples verified the promise of bipolar host materials in PHOLEDs. For example, Yang *et al.* reported that a triphenylamine/oxadiazole-based hybrid bipolar host material (*m*-TPA-*o*-OXD) which served as a host of the green emitter $(ppy)_2$Ir(acac) imparted an external quantum efficiency of 23.7%, and power efficiency of 101 lm W^{-1}.[12] Chou and Cheng designed and synthesized a hybrid carbazole/phosphine oxide-based bipolar host material (BCPO), exhibiting a high glass transition temperature of 137 °C and triplet energy ($E_T = 3.01$ eV).[13] Green PHOLED employing the BCPO host of the green dopant $Ir(ppy)_3$ was obtained with a relatively low turn-on voltage of 2.1 V and maximum external quantum/current/power efficiencies of 21.6%/83.4 cd A^{-1}/87.5 lm W^{-1} respectively. In addition, Kido *et al.* developed a bipolar host material by combining carbazole and pyridine, exhibiting high T_g (102 °C) and triplet energy ($E_T = 2.71$ eV),[14,15] giving a green PHOLED doped with $Ir(ppy)_3$ with maximum external quantum and power efficiency of 26.9% and 102 lm W^{-1} respectively. Furthermore, Yang *et al.* utilized a Si atom as a saturated bridge to link triphenylamine (D) and benzimidazole (A) moieties, giving a novel bipolar host *p*-BISiTPA, in which the π-conjugation is efficiently confined on the individual components.[16,17] The green PHOLED

[a]*Department of Photonics Engineering, Yuan Ze University, Chung-Li, 32003, Taiwan. E-mail: chc@saturn.yzu.edu.tw; Fax: +886-3-4514281; Tel: +886-3-4638800 ext. 7517*
[b]*Department of Chemistry, National Taiwan University, Taipei, 10617, Taiwan. E-mail: kenwong@ntu.edu.tw; Fax: +886-2-33661666; Tel: +886-2-33661667*
[c]*Universal Display Corporation, 375 Phillips Blvd., Ewing, NJ, 08618, USA*
[d]*Center for Organic Photonics and Electronics Research (OPERA), Kyushu University, Motooka 744, Nishi, Fukuoka, 819-0395, Japan*

employing *p*-BISiTPA as the host and $(ppy)_2Ir(acac)$ as the green dopant exhibits maximum external quantum/power efficiencies of 22.7%/72.4 lm W^{-1}. Besides, triazine was also adopted as the acceptor component of bipolar hosts, for example, Adachi *et al.* reported a bipolar host material (TRZ-3Cz) comprised of triazine and carbazole moieties.[18] By employing TRZ-3Cz as the host and $Ir(ppy)_3$ as the dopant, the green PHOLED was obtained with maximum external quantum efficiency as high as 10.2% and power efficiency of 14 lm W^{-1}. Obviously, the device performances employing triazine-embedded bipolar host materials largely lag behind as compared to those of other bipolar systems. In addition, to the best of our knowledge, bipolar host materials incorporating triazine as the electron deficient moiety have not been much exploited for green PHOLEDs devices.[8,19] Furthermore, from the device aspect, the multiple-layer architecture possesses several merits such as energy-barrier reduction, carrier balance, and exciton confinement. However, the inevitable demands of various functional materials may raise the production cost, rendering the PHOLED-based display less competitive as compared to other display technologies. Therefore, it is pertinent to simplify the device configuration of OLEDs without compromising the performance.[20,21]

In this paper, we report the synthesis, characterization, and PHOLED applications of a new bipolar host material, 9-(4,6-diphenyl-1,3,5-triazin-2-yl)-9′-phenyl-3,3′-bicarbazole (**CzT**), which combines the *N*-phenylcarbazole moiety as the electron donor (D) and the 1,3,5-triazine moiety as the electron acceptor (A). The molecular design of **CzT** is based on the following considerations: (1) carbazole is chemically stable itself and can be easily modified at the 3-, 6-, or 9- position. In addition, a phenyl group attached to the 9-position of carbazole can improve the thermal and morphological stabilities. (2) The moderately high oxidative potentials of carbazole-containing compounds make them promising as hole-transport materials. Furthermore, the high triplet energy level of carbazole makes carbazole-cored materials efficient host materials for phosphors. (3) Since triazine has an electron affinity larger than those of other typical electron-deficient heteroaromatic rings (*e.g.*, pyridine, pyrimidine), triazine derivatives are usually utilized as electron injection/transport layers in OLEDs. The combination of the structural features and properties of the carbazole and triazine units endows **CzT** with a balanced transporting behavior for both hole and electron, rendering **CzT** suitable as a bipolar host material. When **CzT** was used as the host material doped with the green phosphorescent emitter $(TPm)_2Ir(acac)$,[22] a triple-layer device gave maximum external quantum/current/power efficiencies of 20.0%/75.7 cd A^{-1}/71.3 lm W^{-1}, respectively. The promising characteristics of **CzT** allow the device architecture further simplified to a double-layer configuration, giving comparable maximum external quantum/current/power efficiencies of 20.1%/76.3 cd A^{-1}/72.7 lm W^{-1}, respectively.

Results and discussions

Scheme 1 displays the synthetic route towards **CzT**. The key intermediate, 3-(9-phenyl-carbazol-3-yl)-9*H*-carbazole (**3**), was synthesized in 74% yield through Suzuki coupling reaction of 3-iodo-9*H*-carbazole (**2**)[23] and the carbazole-based boronic ester (**1**),[24] while **CzT** was obtained in 75% yield after treating

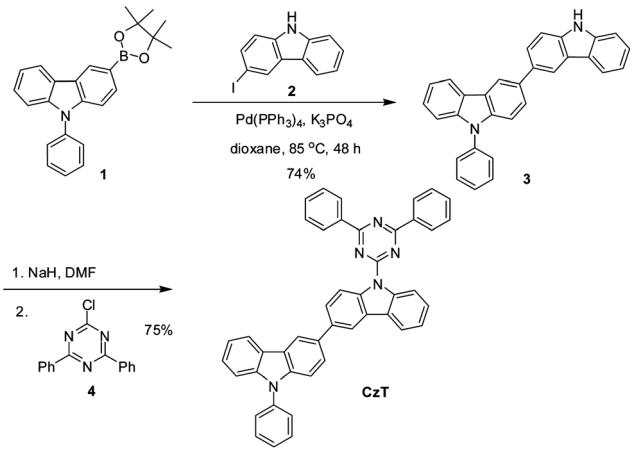

Scheme 1 Synthetic pathways toward the bipolar host **CzT**.

2-chloro-4,6-diphenyl-1,3,5-triazine (**4**) with 3-(9-phenyl-carbazol-3-yl)-9*H*-carbazole (**3**) in the presence of NaH in DMF at room temperature. The chemical structures of **CzT** including intermediates were characterized by ^1H and ^{13}C NMR spectroscopy, mass spectroscopy, and elemental analysis (Experimental section).

We used differential scanning calorimetry (DSC) and thermogravimetric analysis (TGA) to study the morphological properties and thermal stabilities of **CzT**. Because of the molecular configuration of **CzT** with adequate rigidity and steric hindrance, we observed a well-defined glass transition temperature (T_g) of 134 °C, a crystallization peak (T_c = 249 °C), and a melting peak (T_m = 267 °C). The high decomposition temperature (T_d = 425 °C, corresponding to 5% weight loss) showed that **CzT** also exhibits good thermal stability. As a result, **CzT** is capable of forming homogeneous and stable amorphous films upon thermal evaporation.

Fig. 1 depicts the UV-Vis absorption and photoluminescence spectra of **CzT** in dilute dioxane solution. Absorption peaks appeared at 273 and 334 nm and the photoluminescence (PL) spectrum of **CzT** exhibited a maximum peak at 526 nm. For unambiguously determining the triplet energy of **CzT**, a 3 wt% **CzT**:mCP film was prepared, and the delayed PL spectrum (Fig. 1) was captured at the time range between 1.2 and 8.30 ms

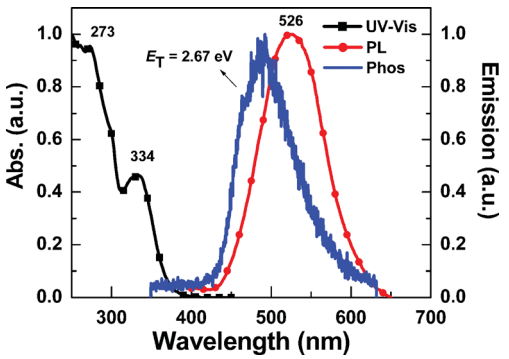

Fig. 1 Room-temperature absorption (UV-Vis) and emission (PL) in dioxane solution, and phosphorescence (Phos) of a 3 wt% **CzT**:mCP film at 9 K.

at 9 K, giving a triplet energy of 2.67 eV which is sufficient for confining green phosphors. The phosphorescence spectrum of **CzT** is blue-shifted as compared to the fluorescence. This result indicates that the triplet state of **CzT** is localized on a specific structural block, while the singlet state is originated from a charge-transfer state,[25] which can be confirmed by the solvent polarity-dependent emission spectra shown below.

The PL quantum yield (PLQY) of **CzT**, determined by an integrating sphere (Hamamatsu C9920) is 6% in dioxane. The low PLQY implies that the efficient non-radiation processes dominate the deactivation of the excited state. The observed large Stokes shift indicates a possible conformational change upon photoexcitation. Since **CzT** is composed of donor and acceptor subunits, emission from a photoexcited intramolecular charge transfer (ICT) can also account for the low PLQY and evident Stokes shift. The solvent polarity-independent UV-vis absorption spectra of **CzT** as shown in Fig. 2a indicate that there is no strong charge transfer in the ground state. However, the PL emission spectra of **CzT** show significant red-shifts from low polarity to high polarity solvents along with the decrease of emission intensity *e.g.* in cyclohexane blue emission (463 nm), to green emission (548 nm) in CH_2Cl_2 (Fig. 2b). This is the strong signature of the polar excited state attributed to the photo-induced charge transfer from the dicarbazole donor to the triazine acceptor.

To understand the electronic structure of **CzT**, density function theory (DFT) calculations were performed at a B3LYP/6-31G(d) level for the geometry optimization. Fig. 3 shows that the HOMO orbital of **CzT** is mainly populated over the dicarbazole and peripheral phenyl moiety, while the LUMO orbital is mainly localized on electron-deficient triazine and its phenyl substitutions. This result reveals that **CzT** has evident spatial separation

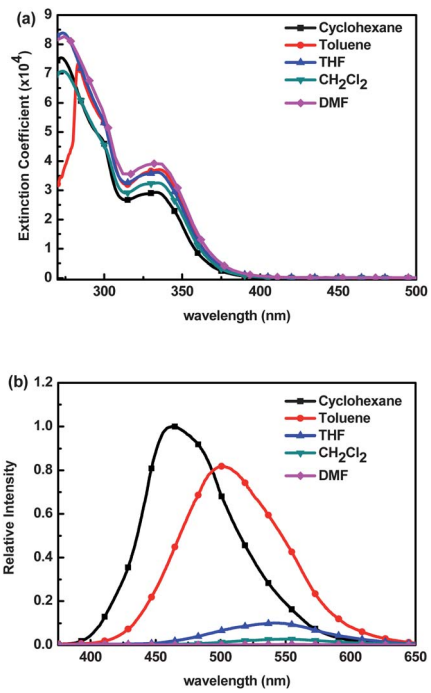

Fig. 2 Absorption (a) and photoluminescence spectra (b) of 2×10^{-5} M **CzT** in different solvents.

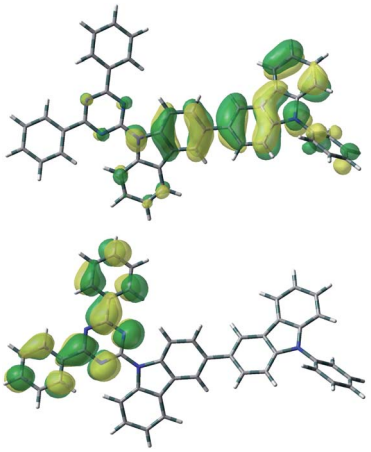

Fig. 3 Frontier molecular orbitals HOMO (top) and LUMO (bottom) of **CzT** calculated with DFT on a B3LYP/6-31G(d) level.

of HOMO and LUMO at hole and electron transporting moieties, respectively, which is beneficial for efficient hole and electron-transporting properties (bipolar). Theoretical analysis agrees with our observation on the solvent-polarity-dependent PL from a polarized excited state due to the electron density distribution shifting from dicarbazole to the triazine moiety upon electronic excitation of **CzT**.

Fig. 4 reveals the bipolar electrochemical character of **CzT**, as evidenced by using cyclic voltammetry (CV). The oxidation/reduction potentials were measured in DMF solution (1.0 mM) containing 0.1 M of *n*-Bu_4NPF_6 as a supporting electrolyte at a scan rate of 100 mV s^{-1}. A glassy carbon electrode and a platinum wire were used as working and counter electrodes, respectively. We observed one quasi-reversible oxidation potential at 1.21 V (onset) and reversible reduction potential at −1.51 V (*vs.* Ag/AgCl). As referred to the reversible oxidation potential of ferrocene/ferrocenium (Fc/Fc^+) redox couple, the HOMO (from the onset oxidation potential) and LUMO (from the half-potential) energy levels of **CzT** were estimated to be −5.49 and −2.77 eV, respectively. The photophysical and electrochemical data of **CzT** are summarized in Table 1.

The bipolar charge carrier transporting property of **CzT** was verified by single carrier devices and compared to a well-known carbazole-based bipolar material, 4,4′-bis(carbazol-9-yl)biphenyl (CBP).[26,27] The hole and electron mobilities of CBP are 2×10^{-3}

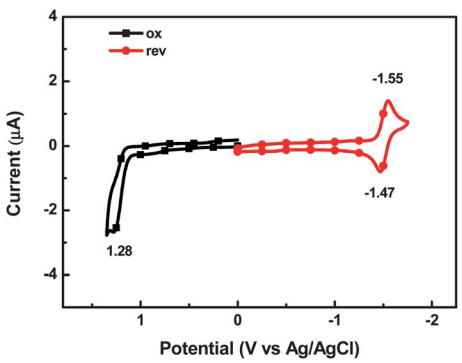

Fig. 4 Cyclic voltammogram of **CzT**.

Table 1 Photophysical and electrochemical data of **CzT** at room temperature

	UV-Vis/nm	PL/nm	Q.Y. (%)	$E_{g,UV}$/eV	$E_{1/2}^{ox}$/V	$E_{1/2}^{red}$/V	T_g/°C	T_c/°C	T_m/°C	T_d/°C
CzT	273, 300 (sh), 334	526	0.06	3.0	1.21	−1.51	134	249	267	425

and 3×10^{-4} cm^2 V^{-1} s^{-1}, respectively, at the applied field of 0.5 MV cm^{-1}. The CBP-based single carrier devices were utilized for probing the carrier transport behavior of **CzT**. The architecture of the hole-only devices was designed as: ITO/PEDOT:PSS (~30 nm)/**CBP** or **CzT** (150 nm)/Au (20 nm)/Al (150 nm), whereas the electron-only devices were composed of ITO/Al (20 nm)/CBP or **CzT** (150 nm)/LiF (0.8 nm)/Al (150 nm). The *I–V* curves of the hole-only and electron-only devices are shown in Fig. 5. Obviously, the experimental outcomes indicate that the current densities of **CzT**-based devices were significantly higher than those of CBP ones. Consequently, **CzT** possesses superior carrier transport properties for both positive and negative charges.

Encouraged by the observed bipolar transport capability of **CzT**, green phosphorescent iridium complexes $Ir(ppy)_3$[13] and $(TPm)_2Ir(acac)$[22] were selected to combine with the bipolar host **CzT** in the host–guest system. We fabricated trilayer devices (devices A) with the architecture as: ITO/TAPC (40 nm)/**CzT** doped with 8 wt% of iridium complex (20 nm)/TmPyPB (50 nm)/LiF (0.5 nm)/Al (150 nm), where di-[4-(*N*,*N*-ditolyl-amino)-phenyl] cyclohexane (TAPC) and 1,3,5-tri[(3-pyridyl)-phen-3-yl] benzene (TmPyPB) were introduced as the hole-transport layer (HTL) and electron-transport layer (ETL), respectively.[28–30] Both TAPC and TmPyPB possess a wide triplet energy gap for preventing the exciton diffusion, high carrier mobility, and suitable HOMO and LUMO levels matching the **CzT** host. The chemical structures of the OLED materials and the schematic structures of the devices are shown in Fig. 6.

The electroluminescence (EL) characteristics of devices A are shown in Fig. 7 and Table 2. The EL spectra of green devices suggested that the emissions were exclusively derived from the emitters, indicating that the emissive excitons are confined on the phosphorescent guests. Device A1 incorporated with $Ir(ppy)_3$ showed an external quantum efficiency of 14%. However, the triplet energy of **CzT** may not be sufficiently high to completely suppress the reverse energy transfer of $Ir(ppy)_3$ back to the host, leading to some energy loss. This assumption can be further verified by using an emitter with a wider gap. Once the commonly used sky-blue phosphor, iridium(III) bis[(4,6-di-fluorophenyl)-pyridinato-*N*,$C^{2'}$]picolinate (FIrpic),[4] was adopted (device A2), the peak external quantum efficiency decreased to about 10%. The broad EL spectrum in device A2 indicates that the excitons are possibly diffused back to the host. In a sharp contrast, device A3 incorporated yellowish-green $(TPm)_2Ir(acac)$ which exhibited

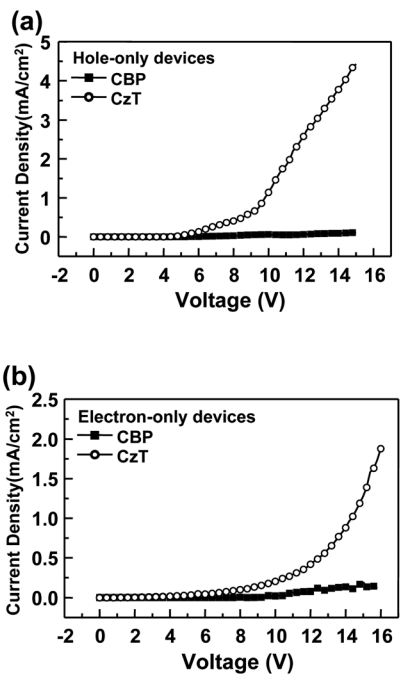

Fig. 5 Current–voltage (*I–V*) characteristics of the hole-only and electron-only devices.

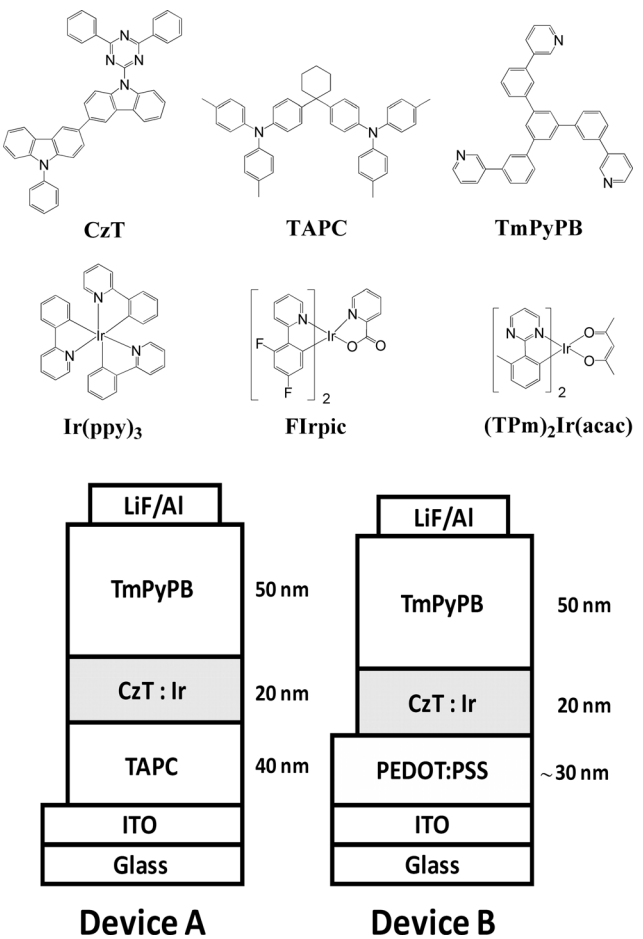

Fig. 6 The structural drawing of materials used in OLEDs and the schematic structures of devices.

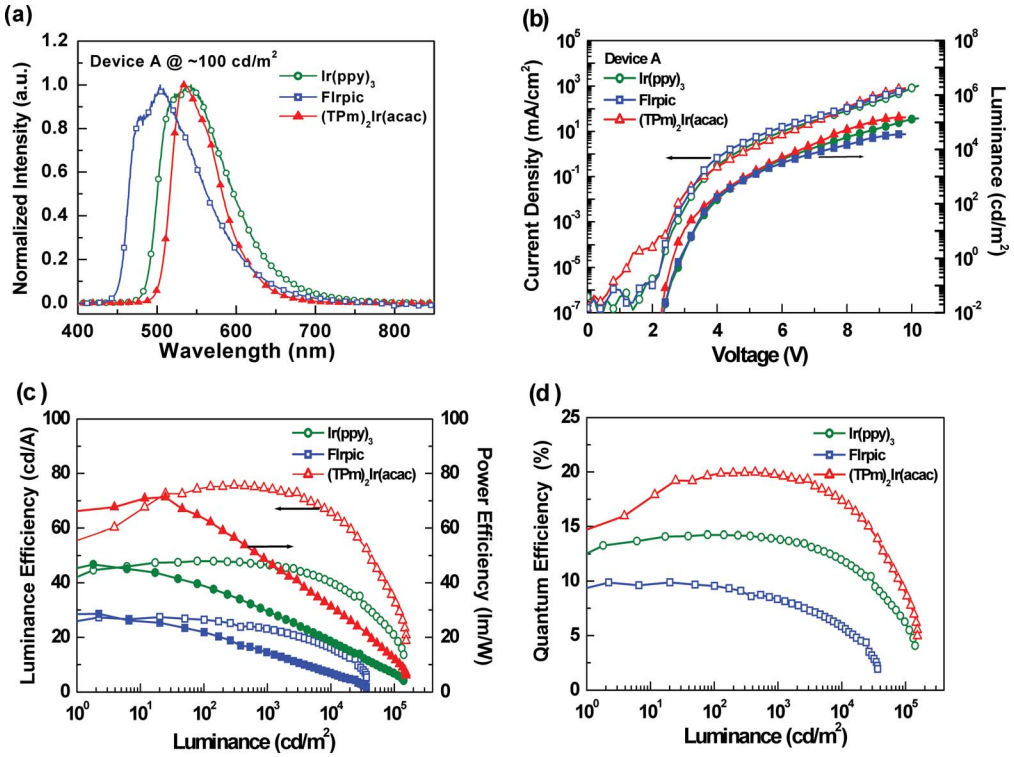

Fig. 7 The electroluminescence characteristics of device A: (a) the normalized EL spectra, (b) current–voltage–luminance (*I–V–L*) characteristics, (c) luminance efficiency/power efficiency *versus* luminance, and (d) external quantum efficiency *versus* luminance for the devices.

an EL with the CIE coordinate of (0.38, 0.59) at 10^2 cd m^{-2}. The maximum external quantum/luminance/power efficiencies of device A3 were up to 20%, 75.7 cd A^{-1}, 71.3 lm W^{-1}, respectively. Without a specific optical structure tuning, the efficiencies imply that a high internal quantum efficiency in device A3 is due to the balanced charge flux and effective confinement of emissive excitons within the emitting layer. The careful molecular design imparts **CzT** with favorable characteristics to serve as an efficient host material of yellowish-green phosphors.

In addition, in view of the energy-level alignments, the HTL and ETL could effectively reduce the excessive carrier leakage and improve the charge carriers recombination zone over the whole emitting layer. Furthermore, the bipolar property of **CzT** with suitable energy levels also helps to facilitate the charge carriers injections from the neighbouring layers, resulting in a low turn-on voltage of 2.6 V. Upon increasing the practical brightness to 10^2 cd m^{-2} (and 10^3 cd m^{-2}) the external quantum/luminance/power efficiencies of device A3 remain 19.8% (19.7%), 74.6 cd A^{-1} (74.5 cd A^{-1}) and 63.6 lm W^{-1} (48.0 lm W^{-1}), respectively. Apparently, this result clearly demonstrates that PHOLEDs utilizing an appropriate bipolar host material are beneficial for reducing efficiency roll-offs. It is noteworthy that the luminance of device A3 reaches to a maximum of 153 009 cd m^{-2} at an operation voltage of 9.8 V.

We envisioned that the HOMO of **CzT** may be suitable for direct hole injection, the conductive polymer, PEDOT:PSS, consequently combined with ITO as the transparent anode. Therefore, a bilayer device (device B) without the TAPC was fabricated as: ITO/PEDOT:PSS (~30 nm)/**CzT** doped with 8 wt % of $(TPm)_2Ir(acac)$ (20 nm)/TmPyPB (50 nm)/LiF (0.5 nm)/Al (150 nm) (Fig. 6). The EL characteristics of devices B are also summarized in Table 2. The EL spectra and CIE coordinate of device B indicate that the emissive excitons are effectively confined within the emitting layer. In the absence of TAPC, device B exhibited maximum efficiencies of up to 20.1%, 76.3 cd A^{-1}, 72.7 lm W^{-1}, respectively. At a practical brightness of 10^2 cd m^{-2} (and 10^3 cd m^{-2}), the efficiencies remain high at 19.8% (17.2%), 75.1 cd A^{-1} (65.3 cd A^{-1}), and 65.5 lm W^{-1} (45.4 lm

Table 2 EL characteristics of green and red phosphorescent OLEDs

Device		Emitter	EQE (%)			LE/cd A^{-1}			PE/lm W^{-1}			V_{on}	$CIE_{x,y}$	$CIE_{x,y}$
			a	*b*	*c*	*a*	*b*	*c*	*a*	*b*	*c*	*d*	*b*	*c*
Trilayer	A1	$Ir(ppy)_3$	14.3	14.3	13.8	48.0	47.9	46.6	47.2	39.0	29.6	2.9	0.374, 0.584	0.371, 0.585
	A2	FIrpic	9.9	9.6	8.3	27.4	26.5	23.1	30.5	21.9	14.5	2.8	0.258, 0.473	0.258, 0.473
	A3	$(TPm)_2Ir(acac)$	20.0	19.8	19.7	75.7	74.6	74.5	71.3	63.6	48.0	2.6	0.382, 0.594	0.380, 0.599
Bilayer	B	$(TPm)_2Ir(acac)$	20.1	19.8	17.2	76.3	75.1	65.3	72.7	65.5	45.4	2.8	0.369, 0.599	0.364, 0.612

[a] Maximum efficiencies. [b] Measured at a brightness of 100 cd m^{-2}. [c] Recorded at 1000 cd m^{-2}. [d] Turn-on voltage measured at 1 cd m^{-2}.

W^{-1}), respectively. Notable differences in the device characteristics between device A3 and B are the maximum luminance and current density. Device A3 configuring a trilayer architecture incorporates with TAPC to give cascade energy levels for smooth hole injection and a high triplet energy for preventing the emissive excitons quenching by PEDOT:PSS,[31,32] leading to better device performance and stability especially under the high brightness condition.

Conclusions

In conclusion, a new dicarbazole–triazine hybrid bipolar host material **CzT** has been synthesized and characterized. **CzT** exhibits a high glass transition temperature (T_g) of 134 °C and a high decomposition temperature (T_d = 425 °C). Theoretical analysis (DFT) reveals that **CzT** has evident spatial separation of HOMO and LUMO at hole and electron transporting moieties, respectively, which is consistent with the observation on the solvent-polarity-dependent PL from a polarized excited state. The lack of effective donor–acceptor conjugation makes **CzT** suitable for yellowish-green phosphors. The bipolar behavior of **CzT** has been confirmed by CV and hole/electron only devices, giving the chance to keep charge carriers balance in the emitting layer. In addition, by employing **CzT** as the bipolar host for the green phosphor complex, $(Tmp)_2Ir(acac)$, the PHOLEDs demonstrate high performance, with maximum efficiencies of 20.0% (75.7 cd A^{-1} and 71.3 lm W^{-1}) and 20.1% (76.3 cd A^{-1} and 72.7 lm W^{-1}) achieved in trilayer and bilayer device architectures, respectively. The trilayer device shows low efficiency roll-off over a wide brightness range of 10^2 to 10^3 cd m^{-2} because the high triplet energy of TAPC can prevent the emissive excitons quenching by PEDOT:PSS. Our results clearly demonstrate that utilizing an appropriate bipolar host material for PHOLEDs is beneficial for enhancing the performance and stability of devices.

Experimental

Synthesis of 3-(9-phenyl-carbazol-3-yl)-9*H*-carbazole 3

A mixture of 3-iodo-9*H*-carbazole (0.88 g, 3.0 mmol), $Pd(PPh_3)_4$ (165 mg, 0.15 mmol), 9-phenyl-3-(4,4,5,5-tetramethyl-1,3,2-dioxaborolan-2-yl)-9*H*-carbazole (1.29 g, 3.5 mmol) and K_3PO_4 (1.8 g, 8.5 mmol) in dioxane (10 ml) was heated at 85 °C with vigorous stirring for 48 h under argon atmosphere. The mixture was poured into water and extracted with DCM. The organic extracts were washed with brine and dried over $MgSO_4$. The solvent was removed by rotary evaporation, and the crude residue was recrystallized in DCM to afford a white solid **3** (0.9 g, 74%). ^{1}H NMR (DMSO-d_6, 400 MHz) δ 11.27 (s, 1H, NH), 8.64 (d, J = 1.2 Hz, 1H), 8.52 (s, 1H), 8.37 (d, J = 7.6 Hz, 1H), 8.22 (d, J = 7.6 Hz, 1H), 7.85–7.80 (m, 2H), 7.72–7.65 (m, 4H), 7.59–7.37 (m, 7H), 7.30 (t, J = 7.6 Hz, 1H), 7.17 (t, J = 7.6 Hz, 1H); ^{13}C NMR (DMSO-d_6, 100 MHz) δ 141.0, 140.7, 139.5, 139.3, 137.4, 134.3, 132.2, 130.6, 128.0, 127.0, 126.7, 126.0, 125.9, 125.4, 123.9, 123.6, 123.4, 123.1, 121.2, 120.8, 120.5, 119.0, 118.8, 118.6, 111.7, 111.5, 110.3, 110.1; MS (*m*/*z*, FAB+) 408 (16.87); HRMS (*m*/*z*, FAB+) calcd for $C_{30}H_{20}N_2$ 408.1626, found 408.1627.

Synthesis of 9-(4,6-diphenyl-1,3,5-triazin-2-yl)-9′-phenyl-3,3′-bicarbazole (CzT)

A solution of sodium hydride (60% in oil, 120 mg, 3.0 mmol) and 3-(9-phenyl-carbazol-3-yl)-9*H*-carbazole (816 mg, 2.0 mmol) in DMF (40 ml) was stirred at room temperature for 1 h under argon atmosphere. 2-Chloro-4,6-diphenyl-1,3,5-triazine (448 mg, 1.67 mmol) was added to the solution at room temperature, then refluxed overnight. The mixture was poured into water and the precipitate was collected by filtration and washed with water, methanol and DCM to get yellow solid **CzT** (800 mg, 75%). Mp: 267 °C (DSC); ^{1}H NMR ($C_2D_2Cl_4$, 400 MHz) δ 9.18 (d, J = 8.8 Hz, 1H), 9.15 (d, J = 8.4 Hz, 1H), 8.76 (dd, J = 7.8 Hz, J = 1.6 Hz, 4H), 8.51 (s, 1H), 8.36 (s, 1H), 8.29 (d, J = 7.6 Hz, 1H), 8.18 (d, J = 7.2 Hz, 1H), 7.98 (d, J = 8.4 Hz, 1H), 7.84 (dd, J = 8.4 Hz, J = 1.6 Hz, 1H), 7.73–7.64 (m, 11H), 7.56–7.47 (m, 5H), 7.40–7.35 (m, 1H); ^{13}C NMR ($C_2D_2Cl_4$, 100 MHz) δ 172.2, 164.8, 141.1, 140.0, 139.3, 137.8, 137.3, 137.0, 135.9, 133.1, 132.75, 129.9, 129.0, 128.8, 127.4, 127.2, 127.0, 126.7, 126.5, 126.4, 126.2, 125.6, 123.7, 123.4, 123.2, 120.4, 120,2, 120.1, 119.7, 118.7, 117.8, 117.7, 110.1, 109.9; MS (*m*/*z*, FAB+) 639 (44.69); HRMS (*m*/*z*, FAB+) calcd for $C_{45}H_{29}N_5$ 639.2423, found 639.2416; anal. calcd C, 84.48; H, 4.57; N, 10.95, found C, 84.31; H, 4.15; N, 10.93.

Photophysics measurements

Samples were purged with nitrogen and recorded in dilute dioxane solution at RT. UV-Vis absorption spectra were recorded using a Hitachi U2800A spectrophotometer. PL spectra were recorded using a Hitachi F9500 fluorescence spectrophotometer. Solution PLQY was determined using a calibrated integrating sphere system (Hamamatsu C9920). The PL spectrum of a 3 wt% **CzT**:mCP film at 9 K was measured using a streak camera system (C4334, Hamamatsu Co.) equipped with a cryostat (GASESCRT-006-2000, IWATANI Co.) A nitrogen gas laser (MNL200, LASERTECHNIK BERLIN) with an excitation wavelength of 337 nm was used.

Cyclic voltammetry

The oxidation/reduction potentials were measured by cyclic voltammetry (CV) in DMF solution (1.0 mM) containing 0.1 M of tetra-*n*-butylammonium hexafluorophosphate ($TBAPF_6$) as a supporting electrolyte at a scan rate of 100 mV s^{-1}. A glassy carbon electrode and a platinum wire were used as working and counter electrodes, respectively. Ferrocene/ferrocenium (Fc/Fc^+) redox couple in DMF/$TBAPF_6$ occurs at E_o = +0.52 V for oxidation and reduction *vs.* Ag/AgCl (sat'd). All potentials were recorded *versus* Ag/AgCl (sat'd) as a reference electrode.

OLED device fabrication

All purchased compounds were subjected to temperature-gradient sublimation under high vacuum before use. OLEDs were fabricated on the indium-tin-oxide (ITO)-coated glass substrates (≤15 Ω) with multiple organic layers sandwiched between the transparent bottom ITO anode and the top metal cathode. The organic and metal layers were deposited by thermal evaporation in a vacuum chamber with a base pressure of $<10^{-6}$ torr. The deposition rate of organic layers was kept at ~0.1 nm

s^{-1}. The conducting polymer, PEDOT:PSS (Clevos PVP CH8000, H. C. Strack), was deposited by spin-coating. The deposition system permitted the fabrication of a complete device structure in a single pump-down without breaking vacuum. The active area of the device was 2×2 mm^2, as defined by the shadow mask for cathode deposition. Current–voltage–luminance (*I–V–L*) characterization of the devices was measured using an Agilent 4156C semiconductor parameter analyzer equipped with a calibrated Si-photodiode. EL spectra of devices were collected by using an Ocean Optics spectrometer.

Acknowledgements

The authors gratefully acknowledge the financial support from National Science Council of Taiwan (NSC 99-2221-E-155-035-MY3, 98-2119-M-002-007-MY3) and Ministry of Economic Affairs (100-EC-17-A-08-S1-042).

Notes and references

1 S. Reineke, F. Lindner, G. Schwartz, N. Seidler, K. Walzer, B. Lüssem and K. Leo, *Nature*, 2009, **459**, 234.
2 C.-H. Chang, K.-C. Tien, C.-C. Chen, M.-S. Lin, H.-C. Cheng, S.-H. Liu, C.-C. Wu, J.-Y. Hung, Y.-C. Chiu and Y. Chi, *Org. Electron.*, 2010, **11**, 412.
3 A. Baldo, D. F. O'Brien, Y. You, A. Shoustikov, S. Sibley, M. E. Thompson and S. R. Forrest, *Nature*, 1998, **395**, 151.
4 C. Adachi, M. A. Baldo, M. E. Thompson and S. R. Forrest, *J. Appl. Phys.*, 2001, **90**, 5048.
5 L. Xiao, S.-J. Su, Y. Agata, H. Lan and J. Kido, *Adv. Mater.*, 2009, **21**, 1271.
6 W. S. Jeon, T. J. Park, S. Y. Kim, R. Pode, J. Jang and J. H. Kwon, *Org. Electron.*, 2009, **10**, 240.
7 A. Benor, S.-Y. Takizawa, C. Pérez-Bolivar and P. Anzenbacher, *Appl. Phys. Lett.*, 2010, **96**, 243310.
8 (*a*) Y. Tao, C. Yang and J. Qin, *Chem. Soc. Rev.*, 2011, **40**, 2943; (*b*) A. Chaskar, H.-F. Chen and K.-T. Wong, *Adv. Mater.*, 2011, **23**, 3876.
9 Y.-L. Liao, C.-Y. Lin, K.-T. Wong, T.-H. Hou and W.-Y. Hung, *Org. Lett.*, 2007, **9**, 4511.
10 W.-Y. Hung, L.-C. Chi, W.-J. Chen, Y.-M. Chen, S.-H. Chou and K.-T. Wong, *J. Mater. Chem.*, 2010, **20**, 10113.
11 L. Duan, J. Qiao, Y. Sun and Y. Qiu, *Adv. Mater.*, 2011, **23**, 1137.
12 Y. Tao, Q. Wang, C. Yang, C. Zhong, J. Qin and D. Ma, *Adv. Funct. Mater.*, 2010, **20**, 2923.
13 H.-H. Chou and C.-H. Cheng, *Adv. Mater.*, 2010, **22**, 2468.
14 S.-J. Su, H. Sasabe, T. Takeda and J. Kido, *Chem. Mater.*, 2008, **20**, 1691.
15 S.-J. Su, C. Cai and J. Kido, *Chem. Mater.*, 2011, **23**, 274.
16 S. Gong, Y. Chen, C. Yang, C. Zhong, J. Qin and D. Ma, *Adv. Mater.*, 2010, **22**, 5370.
17 S. Gong, Y. Chen, J. Luo, C. Yang, C. Zhong, J. Qin and D. Ma, *Adv. Funct. Mater.*, 2011, **21**, 1168.
18 K. S. Son, M. Yahiro, T. Imai, H. Yoshizaki and C. Adachi, *Chem. Mater.*, 2008, **20**, 4439.
19 H.-F. Chen, S.-J. Yang, Z.-H. Tsai, W.-Y. Hung, T.-C. Wang and K.-T. Wong, *J. Mater. Chem.*, 2009, **19**, 8112.
20 P. A. Lane, G. P. Kushto and Z. H. Kafafi, *Appl. Phys. Lett.*, 2007, **90**, 023511.
21 M.-T. Kao, W.-Y. Hung, Z.-H. Tsai, H.-W. You, H.-F. Chen, Y. Chi and K.-T. Wong, *J. Mater. Chem.*, 2011, **21**, 1846.
22 W.-Y. Hung, T.-C. Wang, H.-C. Chiu, H.-F. Chen and K.-T. Wong, *Phys. Chem. Chem. Phys.*, 2010, **12**, 10685.
23 S. H. Tucker, *J. Chem. Soc.*, 1926, **1**, 548.
24 S.-K. Kim, Y.-M. Lee, C.-J. Lee, J.-H. Lee, S.-Y. Oh and J.-W. Park, *Mol. Cryst. Liq. Cryst.*, 2008, 133.
25 F.-M. Hsu, C.-H. Chien, Y.-J. Hsieh, C.-H. Wu, C.-F. Shu, S.-W. Liu and C.-T. Chen, *J. Mater. Chem.*, 2009, **19**, 8002.
26 T. Yamada, F. Suzuki, A. Goto, T. Sato, K. Tanaka and H. Kaji, *Org. Electron.*, 2010, **12**, 169.
27 Z. B. Wang, M. G. Helander, J. Qiu, Z. W. Liu, M. T. Greiner and Z. H. Lu, *J. Appl. Phys.*, 2010, **108**, 024510.
28 L. Xiao, Z. Chen, B. Qu, J. Luo, S. Kong, Q. Gong and J. Kido, *Adv. Mater.*, 2011, **23**, 926.
29 J. Lee, N. Chopra, S.-H. Eom, Y. Zheng, J. Xue, F. So and J. Shi, *Appl. Phys. Lett.*, 2008, **93**, 123306.
30 S.-J. Su, T. Chiba, T. Takeda and J. Kido, *Adv. Mater.*, 2008, **20**, 2125.
31 K. W. Wong, H. L. Yip, Y. Luo, K. Y. Wong, W. M. Lau, K. H. Low, H. F. Chow, Z. Q. Gao, W. L. Yeung and C. C. Chang, *Appl. Phys. Lett.*, 2002, **80**, 2788.
32 U. Giovanella, P. Betti, C. Botta, S. Destri, J. Moreau, M. Pasini, W. Porzio, B. Vercelli and A. Bolognesi, *Chem. Mater.*, 2011, **23**, 810.

